

The possible origin of incommensurate spin textures in HTSC

K.V. Mitsen^a and O.M. Ivanenko

Lebedev Physical Institute RAS, 119991 Moscow, Russia

Received 7 September 2005 / Received in final form 16 May 2006

Published online 31 July 2006 – © EDP Sciences, Società Italiana di Fisica, Springer-Verlag 2006

Abstract. An model of $\text{La}_{2-x}\text{Sr}_x\text{CuO}_4$ explaining the features of incommensurate spin textures without any assumption of stripe formation is proposed. The foundations of this model are the mechanism of negative-U center formation proposed earlier and the concept of specific ordering of doped ions. It is shown that within the framework of the proposed model the features of “stripe” textures of $\text{La}_{2-x}\text{Sr}_x\text{CuO}_4$ reflect exclusively the geometrical relations existing in a square lattice and the competition between different types of doped hole ordering.

PACS. 74.20.Mn Nonconventional mechanisms (spin fluctuations, polarons and bipolarons, resonating valence bond model, anyon mechanism, marginal Fermi liquid, Luttinger liquid, etc.) – 74.72.Dn La-based cuprates – 75.10.-b General theory and models of magnetic ordering

1 Introduction

The past few years have seen many papers devoted to the study of hole-doped cuprate high- T_c superconductors that in one way or another use the concept of stripes [1–3] to analyze the results of research in this field. This concept presupposes the existence of incommensurate modulation of the spin AFM structure in the form of antiphase domains of antiferromagnetically ordered spins separated by narrow extended stripes of doped holes.

The incommensurate modulation of AFM spin structure is observed in neutron scattering experiments [4] as two incommensurate peaks shifted in relation to AFM vector by $\varepsilon = 1/T$ along the modulation vector. Here, T is the period of the magnetic structure in units of the lattice constant.

The results of neutron studies [4–10] of the magnetic texture of $\text{La}_{2-x}\text{Sr}_x\text{CuO}_4$ can be summed up in the form of a stripe phase diagram (Fig. 1a). It is seen that the incommensurate elastic-scattering peaks related to static modulation (shaded areas in Fig. 1a) are observed at $x \leq 0.07$. In the range $0.07 < x < 0.15$ incommensurate peaks are observed in inelastic neutron scattering, which are evidence of dynamic modulation of spin texture (open areas in Fig. 1a). At $x < 0.07$ there are one-dimensional “diagonal” stripes with a single modulation vector directed along orthorhombic axis b , while at $x > 0.05$ there is modulation in two directions parallel to the tetragonal axes (“parallel” stripes). To compare the spin structures for the cases of diagonal and parallel stripes, the diagonal

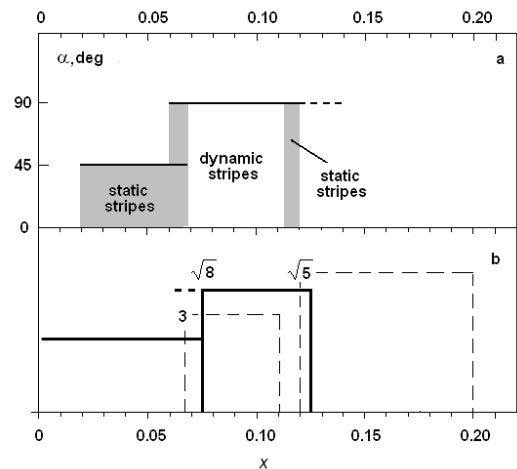


Fig. 1. Experimental magnetic phase diagram of $\text{La}_{2-x}\text{Sr}_x\text{CuO}_4$ [4–10] $\alpha = 45^\circ$ and 90° correspond to diagonal and vertical stripes, respectively. Hatched regions are the intervals where static stripes are observed. (b) Calculated stripe phase diagram of $\text{La}_{2-x}\text{Sr}_x\text{CuO}_4$. The dashed lines bound the regions of percolation along NUC chains with $l_{com} = 3$ and $l_{com} = \sqrt{5}$ (dynamic stripes); the thick lines correspond to the regions of the existence of microdomains with doped Sr ions ordered into a $\sqrt{8} \times \sqrt{8}$ lattice ($0.05 < x < 0.12$) and diagonal lines of Sr ions ($x < 0.066$).

stripes are examined in tetragonal units, too. Thus the spin modulation incommensurability parameter $d = \varepsilon$ for parallel and $d = \varepsilon/\sqrt{2}$ for diagonal stripes.

^a e-mail: mitsen@sci.lebedev.ru

The theory, however, faces significant difficulties in describing the entire set of experimental results. The chief ones are:

1. the relation $d \approx x$ for $x < 0.12$ and $d \approx \text{const.}$ for $x > 0.12$;
2. the transition from diagonal to parallel stripes at $x \approx 0.05$;
3. the change from static to dynamic stripes at $x \geq 0.07$ and emergence of static correlations within a narrow region of concentrations at $x \approx 0.12$ (“pinning of stripes”);
4. the one-dimensionality of diagonal stripes and the two-dimensionality of parallel stripes;
5. the slant of parallel stripes;
6. $2c$ -period of stripe modulation in c -direction (c — is the distance between CuO_2 planes).

In an attempt to explain the results of neutron experiment Gooding et al. [11, 12] proposed the spin-glass model based on the supposition of chaotic distribution of localized doped holes. A localized doped hole is supposed to generates a long-range field of spin distortions of AFM background that can be described as the creation of a topological excitation, a skyrmion [13, 14], with topological charge $Q = \pm 1$ corresponding to twisting of AFM order parameter in the vicinity of a localized hole. Thus, doping destroys long range AFM order and leads to the formation of AFM-ordered microdomains whose angular points are specified by doped holes.

Combining some ideas from [11, 12] together with our ideas concerning the mechanism of two-atomic negative-U center (NUC) formation [15] and Sr ordering (see below) we provide below an alternative explanation of the observed spin and charge modulations.

2 Formation of negative-U centers

We base our reasoning on the assumption that at sufficient low temperatures, the doped holes are rigidly localized in the immediate vicinity of an impurity ion. More precisely, in $\text{La}_{2-x}\text{Sr}_x\text{CuO}_4$ a hole is localized in the CuO_2 plane on four oxygen ions belonging to an oxygen octahedron adjacent to Sr ion (Fig. 2a). This conclusion follows from the results of measurements of X-ray absorption fine-structure (XAFS) spectra [16] and NMR spectra [17] in $\text{La}_{2-x}\text{Sr}_x\text{CuO}_4$.

In accordance with [15] NUC is formed under doping in the CuO_2 plane on a pair of neighboring interior Cu ions belonging to Cu_4O_n cluster (Fig. 2) if two holes formed as a result of doping (doped holes) are localized in the oxygen squares surrounding outer Cu ions (Figs. 2b, 2d). This requirement is fulfilled when the distance between the outer Cu ions (or between the projections of Sr ions onto the CuO_2 plane, which is the same) is $3a$ or $a\sqrt{5}$, where a is the lattice constant in the CuO_2 plane (Figs. 2b, 2d). In the intermediate case, when the distance between outer Cu ions is $a\sqrt{8}$ (Fig. 2c), there is no pair of neighboring copper ions with a doped hole adjacent to each of them, and NUCs are not formed.

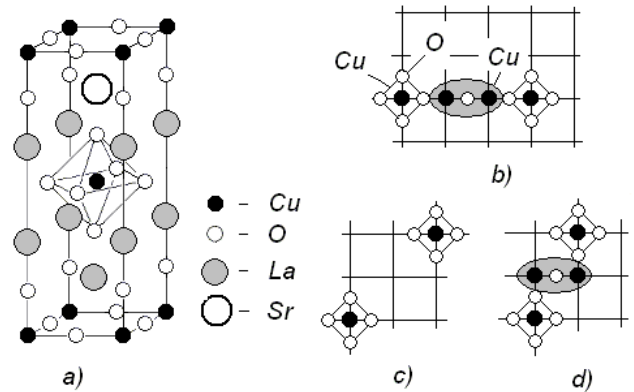


Fig. 2. Formation of NUC in $\text{La}_{2-x}\text{Sr}_x\text{CuO}_4$. (a) Unit cell of $\text{La}_{2-x}\text{Sr}_x\text{CuO}_4$. NUC (dashed oval) is formed on the interior pair of Cu ions in CuO_2 plane if the distance between outer Cu ions (see text) is $3a$ (b) or $a\sqrt{5}$ (d). In the intermediate case, when the distance between Cu ions is $a\sqrt{8}$ (c), there is no pair of neighboring copper ions with a doped hole adjacent to each of them, and NUCs are not formed. This situation corresponds to an insulator.

Pair hybridization of oxygen $p_{x,y}$ -states with NUC states determines the behavior of high- T_c superconductors. Electron pairing in such system, responsible for high- T_c superconductivity, emerges because of strong renormalization of the effective electron-electron interaction when scattering with intermediate virtual bound states of NUC's is taken into account.

Thus, doped carriers in our model are localized, and they are responsible for the formation of NUC's. These NUC's act as pair acceptors and generate additional hole pairs, which are also localized in the vicinity of the NUC. Conduction occurs in such a system if these regions of hole localization form percolation clusters in CuO_2 plane and by means of quantum tunneling between such clusters. As well, conductivity can be provided if isolated clusters of NUC's are imbedded in metal matrix.

3 Ordering of doped holes in $\text{La}_{2-x}\text{Sr}_x\text{CuO}_4$

In the considered scheme of the doping the system of Sr ion and hole located in oxygen sheet, represents an electric dipole that interacts with other dipoles through long range Coulomb potential. In such systems the orientation interaction between dipoles arises, that results in alignment of these dipoles by opposite poles to each other. Based upon crystal structure of $\text{La}_{2-x}\text{Sr}_x\text{CuO}_4$ it is possible to assume that replacement La on Sr will occur so that arising dipoles form vertical chains (remining crankshafts) extended along c -axis (Fig. 3). Such arrangement simultaneously removes a question: what of La(Sr)O planes dopes hole in the central CuO_2 plane.

Let believe that chains are flat and drawn up parallel to each other. The calculation of electrostatic interaction energy of dipole chains shows, that two nearest chains

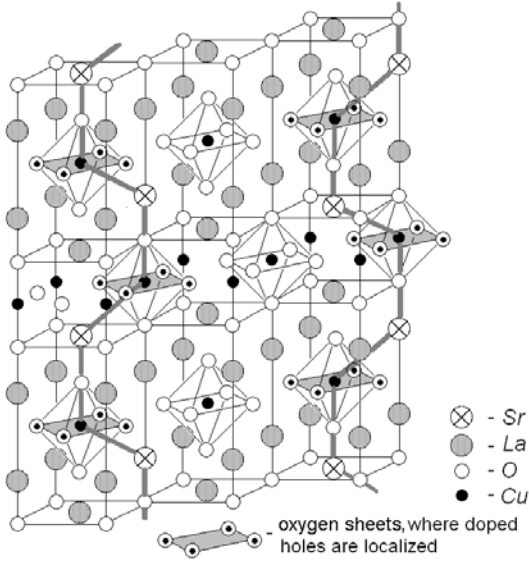


Fig. 3. Ordering of Sr ions in $\text{La}_{2-x}\text{Sr}_x\text{CuO}_4$. Negatively charged strontium ions together with doped holes “ascribed” to them are dipoles that attract each other at opposite ends to form cranked chains.

(Fig. 3) will attract to each other if doped holes are spaced $l_{com} \geq 2$ and the next nearest chains repulse from each other. Such character of interaction results in dipole chain ordering and occupation of the sites in square lattice with certain parameter l_{com} by doped holes. The minimum of interaction energy is appropriate to $l_{com} = \sqrt{8}$. At the same time it is follows from calculation that the energies of configurations with $l_{com} = 2, \sqrt{5}, \sqrt{8}$ and 3 are close with a precision of $\Delta E \sim 10^{-2} e^2 / \varepsilon a \sim 50$ K per dipole ($a = 4 \times 10^{-8}$ cm, ε — is the permittivity). This value is determined the temperature of charge ordering T_{ch} . Above T_{ch} the doped holes localized on oxygen sheets around some Cu ions can jump to next oxygen ions.

Because the energies of configurations with $l_{com} = 2, \sqrt{5}, \sqrt{8}$ and 3 are very close the simultaneous coexistence of microdomains, in which doped holes occupy the sites in square lattices with definite but different l_{com} , is possible. Microdomains with a given l_{com} distance can only exist over a certain concentration x range. This range is bounded from above by the $x_{com} = 1/l_{com}$ value; at higher concentrations, the existence of physically significant domains with given l_{com} violates the condition of a constant mean concentration. At $x < x_{com}$, dipole chains become broken, and vacancies appear in the square lattices of projections. Microdomains with a given l_{com} distance remain intact up to some $x = x_p$ value, which, at a random distribution, corresponds to the two-dimensional percolation threshold $x_p = 0.593$ [18]. That is the percolative cluster serves as a carcass of a given microdomain. Accordingly, the existence of microdomains with given l_{com} is possible in the concentration range satisfying a condition

$$0.593/l_{com}^2 < x \leq 1/l_{com}^2.$$

Table 1. Intervals of the existence for microdomains with various l_{com} values.

l_{com}	x_p	x_m	Properties
>3			insulator
3	0.066	0.111	high- T_c superconductor
$\sqrt{8}$	0.075	0.125	insulator
$\sqrt{5}$	0.12	0.20	high- T_c superconductor
2	0.15	0.25	normal metal

Note: x_p and x_m are the lower and upper boundaries of the concentration range in which domains with the given l_{com} can exist, $x_m = 1/l_{com}^2$; $x_p = 0.593x_m$ is the percolation threshold, when the existence of percolation chains with $l = l_{com}$ becomes possible. The last column contains characteristics of microdomains with the given l_{com} value.

The concentration of occupied sites p in such microdomain changes with x from $p \approx 0.6$ (at $x = 0.593/l_{com}^2$) up to $p = 1$ (at $x = 1/l_{com}^2$).

The size of the ordered microdomain depends on the proximity of x to x_{com} . Along the c -axis the size of the ordered microdomain appears to be of some lattice constants, with the pattern of doped hole ordering being repeated in every second CuO_2 plane.

We assume that, at small x (at a mean distance between dopant projections of $l > 3a$), dipole chains are grouped in planes parallel to the c axis and the orthorhombic a axis in such a way that the distance between doped holes (or strontium ion projections) along the a axis be $a\sqrt{8}$, that is, correspond to minimum interaction energy.

As follows from our reasoning, $\text{La}_{2-x}\text{Sr}_x\text{CuO}_4$ must be treated as a set of mutually penetrating domains in which strontium ions are ordered in such a manner that doped holes fill (in part or completely) square lattice sites with various l_{com} values determined by the concentration. The site percolation regions in lattices with various l_{com} values, that is, the concentration regions corresponding to the existence of clusters of various phases, can be determined. Table 1 lists the existence intervals of domains with different l_{com} .

4 Formation of spin textures

Now we consider the spin textures formed because of dopant ordering. Let us examine the case of complete Sr ordering at $x_{com} = 1/8$. We assume that each hole circulates over the oxygen sheet surrounding a copper ion and that because of the interaction between the hole current and the spins of the four nearest copper ions the latter are polarized. The emerging distortions of the AFM background can be described as the creation of a topological excitation, a skyrmion [13,14], with a topological charge ± 1 corresponding to twisting of the AFM order parameter (Fig. 4) in the vicinity of a localized hole.

Figure 5a shows a possible ordering of the projections of Cu spins on the CuO_2 plane for a completely ordered arrangement of localized holes at $x = 1/8$. Here, the CuO_2

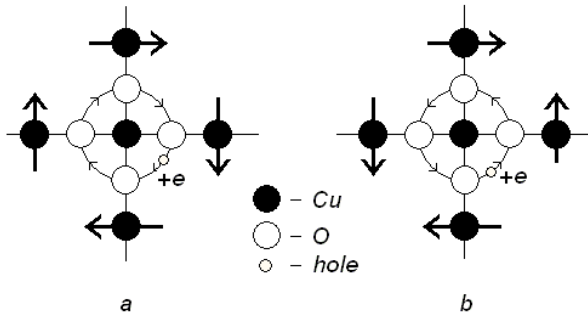


Fig. 4. Rotation of the directions of Cu spin projections in the vicinity of a skyrmion for topological charges $Q = +1$ (a) and $Q = -1$ (b).

plane is broken up into separate AFM-ordered quadrangular microdomains whose corners are determined by the localized doped holes. The directions of Cu spin projections at lattice sites are indicated by arrows. The emerging pattern is characterized by the AFM-ordering of the microdomains proper and by the ordered alternation of skyrmions. Such a checkerboard pattern of AFM-ordered microdomains (Fig. 5a) results in an imitation of a “parallel stripe” structure. Actually, the “parallel stripes” are of the chains antiphase microdomains with magnetization directions along horizontal or vertical axes (Fig. 5a). The magnetic modulation period $T_m = 8$ in this case is equal to the total size of two antiphase microdomains along the modulation vector and a rectangle with an area equal to $2 \times T_m$ must contain two sites. I.e.

$$2T_m x = 2; \quad \text{and} \quad d = 1/T_m = x = 1/8.$$

Thus, the relation $d = x$ in the case of parallel stripes is caused exclusively by the fact that doped holes lie along straight lines equally spaced at $l_{com} = 2$.

Now let us consider the magnetic textures formed at a slight deviation of x below $x_{com} = 1/8$. Kimura et al. [10] used an $\text{La}_{1.88}\text{Sr}_{0.12}\text{CuO}_4$ sample to observe the modulation of a spin texture with an incommensurability parameter $d = 0.118$. This corresponds to a mean texture period $\overline{T_m} \approx 8.5$ (in units of a), i.e., to the alternation of two periods, $T_{m1} = 8$ and $T_{m2} = 9$. Figure 5b shows the picture of an ordered distribution of doped holes we proposed for a mean concentration $x = 0.118$, which was obtained by cutting the completely ordered lattice at $x = 1/8$ along the orthorhombic a -axis and shifting one part in relation to the other by the vector $q = (1, 1)$. Such a dislocation conserves the coherence of ordering in domains on both sides of the dislocation (with a small phase shift). Such a structure (Fig. 5b) produces characteristic reflections in the diffraction pattern, and these reflections correspond to incommensurable modulation of both spin with an incommensurability parameter d . The condition of conservation of the mean concentration yields

$$T_d x_m = (T_d - 1)x_l.$$

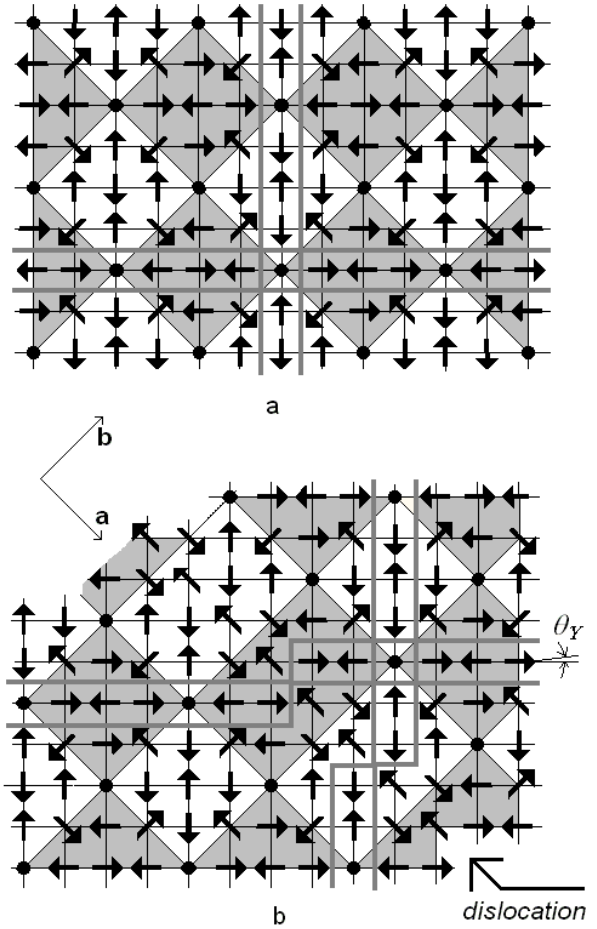


Fig. 5. (a) Projections of spin directions at $x = 1/8$ when doped holes are ordered into a $\sqrt{8} \times \sqrt{8}$ lattice. Microdomains that form horizontal stripes are hatched, thick lines denote stripe directions. (b) The same at $x < 1/8$. The plane is divided into domains separated by diagonal dislocations, which are nuclei of diagonal stripes. The shift of vertical stripes by one cell at each dislocation results in an effective tilt of parallel stripes by the θ_γ angle.

Here T_d is the mean dislocation period in units of a . To maintain the mean concentration $x_m = 0.118$ for a local concentration inside a domain $x_l = 0.125$, the introduced diagonal dislocations must have a mean period $T_d = 17$ ($=T_{m1} + T_{m2}$). Such quasiperiodic dislocations, which lead to incommensurable modulation of the crystal structure and the spin texture, result in incommensurable reflections $d = 0.118$ in full agreement with the experiment [10].

The special feature of the appearing picture of ordering is the shift of parallel stripes by one lattice constant (see Fig. 5b); that is, as though, they deflected from tetragonal axes by the $\theta_\gamma = 1/17 \approx 3.3^\circ$ angle toward the orthorhombic axis b . These are those “slanted” parallel stripes with a slope angle of 3° , which were observed by Kimura et al. [10].

Let us now turn to the case of arbitrary values of x for $x < 0.125$. Here, the distribution pattern can be obtained

from the completely ordered distribution at $x = 0.125$ (Fig. 5a) by removing a certain number of lines of sites one after another. The texture imitating parallel stripes may occur down to $x \approx 0.05$ because small clusters (pieces of broken lines) with $l_{com} = \sqrt{8}$ still survive due to large relative fluctuations of concentration in small volume.

Let us suppose that the lattice contains such correlated remnant fragments of a parallel stripe texture genetically linked to $\sqrt{8} \times \sqrt{8}$ microdomains. The related neutron diffraction pattern exhibits characteristic reflections determined by the mean remnant texture period. In turn, the mean period T of this texture, defined as the distance between the equivalent points of unidirectional magnetic domain, includes two occupied sites. I.e. a rectangle with an area equal to $T_m l_{com} / \sqrt{2} = 2T_m$ must contain two sites and $d = 1/T_m = x$. This relation for parallel stripes takes place at $0.05 < x < 0.125$, when the $\sqrt{8} \times \sqrt{8}$ lattice is occupied.

As is seen from Figure 5b the inserted dislocations are actually the nucleus of diagonal stripes extended along a -axis. They appear as quasi-periodic structures at $x < 0.05$ when $\sqrt{8} \times \sqrt{8}$ texture remainders disappear, and there only remain diagonal lines of impurity dipoles with a distance of $l_{com} \geq 2\sqrt{8}$ between the lines and a distance of $l_{com} = \sqrt{8}$ between the dipoles. Therefore diagonal stripes are always directed along the orthorhombic a -axes and, accordingly, the modulation vector, along the other orthorhombic b -axes. If all dipoles are ordered in diagonal ranks, the period of diagonal spin modulation T_m (in tetragonal axes) should be equal $T_m = 1/\sqrt{2}x$ (or $d = \sqrt{2}x$). Since the part of doped holes can remain in space between dipole ranks the period of observable spin structure will be more, than $1/\sqrt{2}x$, accordingly d is less than $\sqrt{2}x$. The experimental value of d varies [5] from $d \approx 0.7x$ up to $d \approx 1.4x$ over the range $0.01 < x < 0.05$.

The last problem that we will discuss deals with dynamic stripes. Figure 1b shows the concentration ranges within which there can be antiferromagnetically correlated clusters of $\sqrt{8} \times \sqrt{8}$ microdomains ($0.05 < x < 0.125$) and diagonal chains of doped holes spaced $l = \sqrt{8}$ ($x < 0.07$). The dashed lines limit the regions of existence of percolation clusters with $l_{com} = 3$ and $l_{com} = \sqrt{5}$. Such conductive cluster bordering on AFM cluster destroys the static spin correlations because of the motion of charges that disrupt the magnetic order in the neighborhood along its path. Therefore spin correlations can be observed in the range $0.066 < x < 0.11$ only in inelastic neutron scattering as dynamic incommensurable magnetic fluctuations. What is remarkable (see Fig. 1b) is that in addition to the region $x < 0.07$ there is a narrow interval of concentrations $0.11 < x < 0.12$ where there is no percolation along NUC, and it is precisely in this interval that static incommensurable correlations are again observed (Fig. 1a). At nonhomogeneous Sr distribution the existence of small ordered domains with $x \leq 0.125$, bordering a percolative cluster with $l_{com} = \sqrt{8}$, is possible at $x > 0.125$. It results

in the experimental observation of dynamic spin texture with $d \approx 0.125$.

5 Conclusion

Thus we have found that the localization of doped holes and the ordering of the Sr ions in $\text{La}_{2-x}\text{Sr}_x\text{CuO}_4$ in certain lattices can lead to the formation of an incommensurate spin texture, which imitates stripe modulation, with an incommensurability parameter $d = x$. We have discussed in detail the stripe phase diagram of $\text{La}_{2-x}\text{Sr}_x\text{CuO}_4$ in the framework of proposed model and have shown that its features only reflect the geometrical relations existing in a square lattice and the competition of different types of dopant ordering.

The work was supported by Russian Foundation for Basic Research (grant # 05-02-16706).

References

1. J. Zaanen, O. Gunnarsson, Phys. Rev. B **40**, 7391 (1989)
2. K. Machida, Physica C **158**, 192 (1989)
3. S.A. Kivelson, V.J. Emery, H.-Q. Lin, Phys. Rev. B **42**, 6523 (1990)
4. J.M. Tranquada, J.D. Axe, N. Ichikawa, Y. Nakamura, S. Uchida, B. Nachumi, Phys. Rev. B **54**, 7489 (1996)
5. K. Yamada, C.H. Lee, Y. Endoh, G. Shirane, R.J. Birgeneau, M.A. Kastner, Physica C **282–287**, 85 (1997)
6. K. Yamada, C.H. Lee, K. Kurahashi, J. Wada, S. Wakimoto, S. Ueki, H. Kimura, Y. Endoh, S. Hosoya, G. Shirane, R.J. Birgeneau, M. Greven, M.A. Kastner, Y.J. Kim, Phys. Rev. B **57**, 6165 (1998)
7. M. Matsuda, M. Fujita, K. Yamada, R.J. Birgeneau, Y. Endoh, G. Shirane, Phys. Rev. B **65**, 134515 (2002)
8. M. Fujita, K. Yamada, H. Hiraka, P.M. Gehring, S.H. Lee, Phys. Rev. B **65**, 64505 (2002)
9. M. Fujita, H. Goka, K. Yamada, M. Matsuda, Phys. Rev. B **66**, 184503 (2002)
10. H. Kimura, H. Matsushita, K. Hirota, Y. Endoh, K. Yamada, G. Shirane, Y.S. Lee, M.A. Kastner, R.J. Birgeneau, Phys. Rev. B **61**, 14366 (2000)
11. R.J. Gooding, N.M. Salem, A. Mailhot, Phys. Rev. B **49**, 6067 (1994)
12. R.J. Gooding, N.M. Salem, R.J. Birgeneau, F.C. Chou, Phys. Rev. B **55**, 6360 (1997)
13. A.A. Belavin, A.M. Polyakov, Pis'ma Zh. Eksp. Teor. Fiz. **22**, 503 (1975); [JETP Lett. **22**, 245 (1975)]
14. R.J. Gooding, Phys. Rev. Lett. **66**, 2266 (1991)
15. K.V. Mitsen, O.M. Ivanenko, Zh. Eksp. Teor. Fiz. **118**, 666 (2000); [JETP **91**, 579 (2000)]
16. D. Haskel, V. Polinger, E.A. Stern, AIP Conf. Proc. **483**, 241 (1999)
17. P.C. Hammel, B.W. Statt, R.L. Martin, F.C. Chou, D.C. Johnston, S.-W. Cheong, Phys. Rev. B **57**, R712 (1998)
18. R.M. Ziff, Phys. Rev. Lett. **69**, 2670 (1992)